



Research article

A comparative transcriptomics analysis reveals ethylene glycol derivatives of squalene ameliorate excessive lipogenesis and inflammatory response in 3T3-L1 preadipocytes

Yu Cheng^a, Farhana Ferdousi^{a,b,c}, Bryan Angelo Foronda^d, Tran Ngoc Linh^e, Munkhzul Ganbold^e, Akira Yada^{e,f}, Takashi Arimura^e, Hiroko Isoda^{a,b,c,e,*}

^a Tsukuba Life Science Innovation Program (T-LSI), Graduate School of Science and Technology, University of Tsukuba, Tsukuba, Japan

^b Institute of Life and Environmental Sciences, University of Tsukuba, Japan

^c Alliance of Research on the Mediterranean and North Africa (ARENA), University of Tsukuba, Tsukuba, Japan

^d School of Life and Environmental Sciences, University of Tsukuba, Japan

^e National Institute of Advanced Industrial Science and Technology (AIST)-University of Tsukuba Open Innovation Laboratory for Food and Medicinal Resource Engineering (FoodMed-OIL), University of Tsukuba, Tsukuba, Japan

^f Interdisciplinary Research Center for Catalytic Chemistry, National Institute of Advanced Industrial Science and Technology (AIST), Tsukuba Central 5, 1-1-1 Higashi, Tsukuba, 305-8565, Japan

ARTICLE INFO

Keywords:

Microarray analysis
Transcriptome analysis
Adipocyte differentiation
Squalene
Ethylene glycol derivatives
3T3-L1 cells

ABSTRACT

Squalene (SQ) is a natural compound with anti-inflammatory, anti-cancer, and anti-oxidant effects, but due to its low solubility, its biological properties have been greatly underestimated. This study aims to explore the differences in gene expression patterns of four newly synthesized amphipathic ethylene glycol (EG) derivatives of SQ by whole-genome transcriptomics analysis using DNA microarray to examine the mRNA expression profile of adipocytes differentiated from 3T3-L1 cells treated with SQ and its EG derivatives. Enrichment analyses of the transcriptional data showed that compared with SQ, its EG derivatives exerted different, in most cases desirable, biological responses. EG derivatives showed increased enrichment of mitochondrial functions, lipid and glucose metabolism, and inflammatory response. Mono-, di-, and tetra-SQ showed higher enrichment of the cellular component-ribosome. Histological staining showed EG derivatives prevented excessive lipid accumulation. Additionally, mitochondrial transcription factors showed upregulation in tetra-SQ-treated cells. Notably, EG derivatives showed better anti-inflammatory effects. Further, gene-disease association analysis predicted substantial improvement in the bioactivities of SQ derivatives in metabolic diseases. Cluster analyses revealed di- and tetra-SQ had more functional similarities than others, reflected in their scanning electron microscopy images; both di- and tetra-SQ self-organized into similar sizes and shapes of vesicles, subsequently improving their cation binding activities. Protein-protein interaction networks further revealed that cation binding activity might explain a major part, if not all, of the differences observed in functional analyses. Altogether, the addition of EG derivatives may improve the biological responses of SQ and thus may enhance its health-promoting potential.

* Corresponding author. Faculty of Life and Environmental Sciences, University of Tsukuba, Tsukuba, Ibaraki, Japan.
E-mail address: isoda.hiroko.ga@u.tsukuba.ac.jp (H. Isoda).

<https://doi.org/10.1016/j.heliyon.2024.e26867>

Received 1 September 2023; Received in revised form 27 December 2023; Accepted 21 February 2024

Available online 2 March 2024

2405-8440/© 2024 The Authors. Published by Elsevier Ltd. This is an open access article under the CC BY-NC license (<http://creativecommons.org/licenses/by-nc/4.0/>).

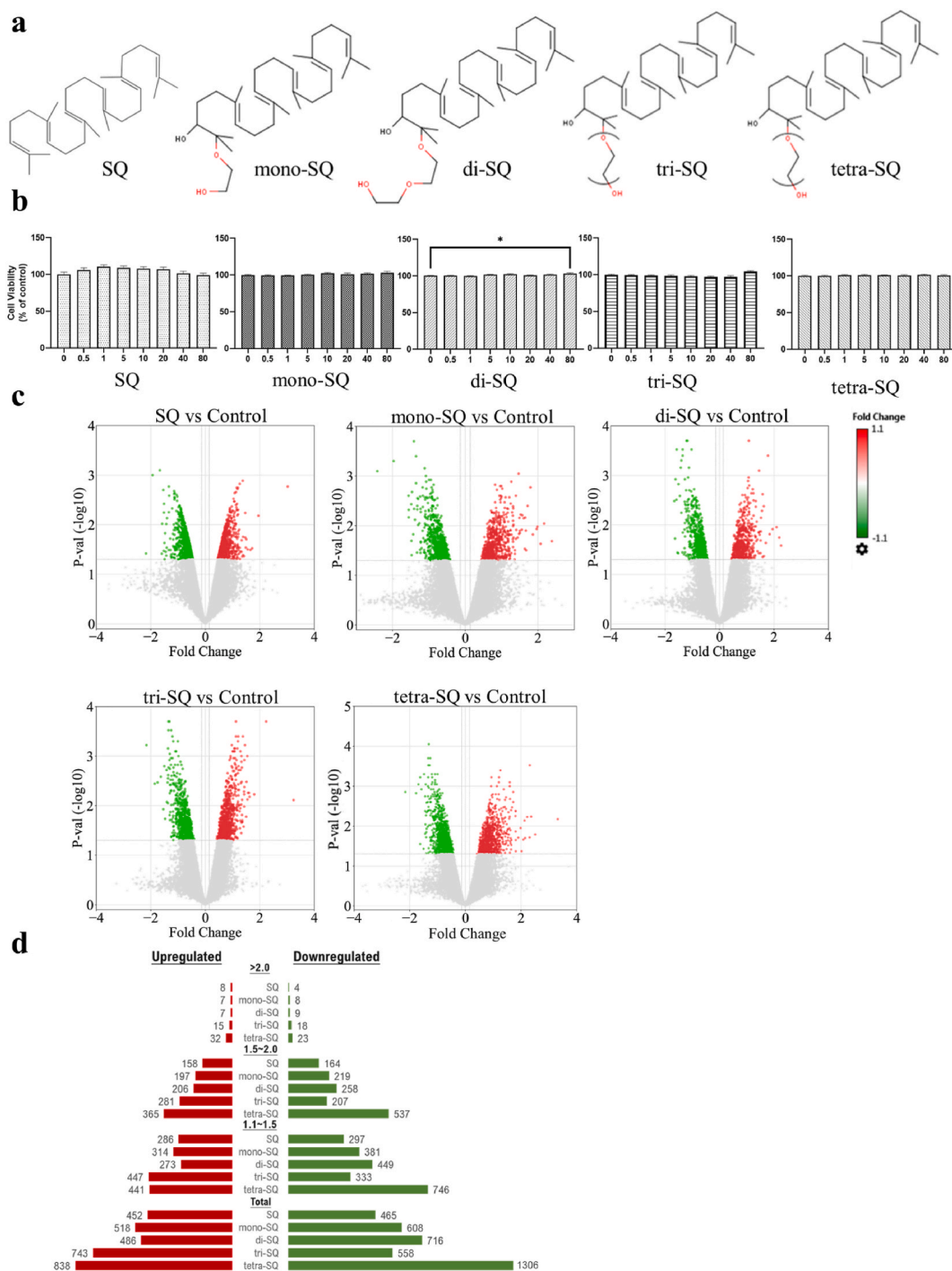


Fig. 1. Gene expression patterns in SQ and EG derivatives treated cells. (a) Chemical structures of SQ and EG derivatives (mono-SQ, di-SQ, tri-SQ, tetra-SQ). (b) Cell viability results after 24-h treatment of SQ and EG derivatives on 3T3-L1 cells, n = 3. *p < 0.05; ANOVA followed by Dunnett's post hoc test. (c) Volcano plot of DEGs between SQ- and EG derivative-treated and control 3T3-L1 cells. The X-axis displays linear fold change, and the Y-axis corresponds to -log10 p-values. Filter criteria for DEGs were set at p-value < 0.05, and -1.1 > fold change > 1.1. The red dots represent the upregulated genes; the green dots represent the downregulated genes. The grey dots represent the genes that did not pass the filter criteria. (d) Bar graphs of fold change distribution of up- and down-regulated DEGs in SQ- and EG derivatives-treated groups.

1. Introduction

Squalene (SQ) is a natural polyunsaturated hydrocarbon, which was first discovered in shark liver fish oil [1,2] and has a wide range of sources, not only from fish liver oil but also in various plant seeds [3,4]. In recent years, due to cost and environmental protection considerations, SQ has also been extracted from microorganisms [5]. SQ plays an important role as a precursor for cholesterol synthesis in animals and plants [6]. According to published results, SQ inhibits not only the superficial tumor but also the growth of tumors of internal organs [7]. In addition, SQ also plays an important role in anti-inflammation [8,9], improving steroid metabolism and cardiovascular and cerebrovascular diseases [10]. However, despite several promising roles of SQ, its applicability to humans has been met with only limited success, largely due to the hydrophobic structure of SQ. Due to the low solubility in water, SQ will accumulate in the serum after oral intake but can not elevate serum cholesterol levels [11], indicating its low bioavailability *in vivo*.

In this regard, structural modifications of natural products have been receiving great attention as the semisynthetic derivatives have been proven valuable sources of new drug candidates with a variety of biological as well as pharmacological activities. For example, polyethylene glycol (PEG)-coated nanoparticles can help improve the efficiency of drug delivery to target cells and tissues [12] and can also be covalently linked to proteins to form derivatives that improve pharmacokinetics [13]. Therefore, finding a method to improve the hydrophobicity of SQ is a good way to improve its utilization *in vivo*.

In our previous efforts to investigate how ethylene glycol (EG) moiety affects the functions of SQ, we found that amphiphilic SQ derivatives can inhibit inflammation by regulating the expression of inflammatory mediators and proinflammatory factors [14,15], and promote lipogenesis by improving glucose homeostasis and energy metabolism [15]. In addition to the proven mono-SQ, the newly synthesized EG derivatives of SQ (di-SQ, tri-SQ, and tetra-SQ) can also overcome the hydrophobic properties of SQ [16]; however, their biological role remains to be confirmed.

In the present study, we aimed to explore the biological activities of EG derivatives of SQ and compare their functionalities with SQ through employing an untargeted whole-genome transcriptomic analysis approach. We examined the effects of SQEGs on gene expression during 3T3-L1 preadipocyte cell differentiation and evaluated their roles in key biological functions, including lipogenesis, lipid accumulation, mitochondrial function, and inflammation.

2. Materials and methods

2.1. Chemicals

SQ was purchased from Tokyo Chemical Industry Co., Ltd. Under the catalysis of Squalene Monooxygenase, SQ reacts with NADPH and molecular oxygen to form 2,3-epoxysqualene. Subsequently, four EG derivatives of SQ (Fig. 1a) were synthesized by adding one to four mono-ethylene glycol moieties to 2,3-epoxysqualene [14,16].

2.2. 3T3-L1 preadipocyte culture and adipogenic differentiation

The 3T3-L1 preadipocytes were seeded to confluency for two days in the induction medium, which was prepared by 1% isobutylmethylxanthine, 1% dexamethasone and 1% insulin. Three days after induction, cells were cultured in a differentiation medium prepared with 1% insulin, treated with 5 μ g SQ or 5 μ g EG derivatives for another 11 days. The differentiation medium was changed every two days.

2.3. Cell viability assay

3T3-L1 preadipocytes were prepared as a single-cell suspension, seeded into 96-well plates at 1000 cells per well and incubated for 24 h. After the cells were treated with SQ or its derivatives for 24 h, 5 mg/mL 3-(4,5-Dimethylthiazol-2-yl)-2,5-diphenyltetrazolium bromide (MTT assay) solution (PBS as solvent, 20 μ L/well) (Dojindo, Kumamoto, JP) was added, and the culture was terminated after continuing to incubate for 4 h. Then, dimethyl sulfoxide (DMSO) was used to dissolve the MTT formazan. The microplate reader (Powerscan HT) was used for soluble formazan measurement at 490 nm absorbance.

2.4. Lipid droplets (LDs) red oil staining

Cells were seeded on glass slides, differentiated with or without SQ and its derivatives, and slides were incubated in propylene glycol for 2 min according to the protocol of the Oil Red O (ORO) Stain Kit (Cayman Chemical, MI, United States). Slides were incubated in ORO solution for 6 min and differentiated again in 85% propylene glycol for 1 min. Slides were then rinsed and incubated in hematoxylin for 1–2 min. Finally, ORO staining of LDs images was obtained using a Leica TCS SP8 confocal microscope.

2.5. RNA isolation and real-time PCR

Total RNA was extracted from mature adipose cells using ISOGEN reagent (Nippon Gene, Tokyo, Japan), and reverse-transcribed using the SuperScriptTM IV VIL0TM Master Mix (Invitrogen, Carlsbad, CA, USA) following the manufacturer's protocols. RNA was reverse transcribed and amplified to obtain single-stranded Complementary DNA (cDNA). NanoDrop 2000 spectrophotometer

(Thermo Fisher Scientific, MA, USA) was used to measure the cDNA concentration. Superscript IV Reverse Transcriptase Kit (Thermo Fisher Scientific, MA, USA) was used for RNA reverse transcription to cDNA, according to manufacturer's instructions. Amplification reactions of cDNA were performed by using the Applied Biosystems 7500 Fast Real-Time PCR System (Thermo Fisher Scientific Inc, MA, USA). Relative expression of mRNA was calculated by 2- $\Delta\Delta C_t$ method and *Gapdh* was selected as an internal reference gene to normalize gene expression. All TaqMan primers (Applied Biosystems) were purchased from ThermoFisher Scientific Inc.

2.6. Microarray analysis

Whole-genome microarray analysis of cells treated with SQ and EG derivatives was performed on Affymetrix's GeneAtlas® System (Affymetrix Inc., Santa Clara, CA, USA), according to instructions provided by the manufacturer. First, total RNA was isolated from 3T3-L1 cells using ISOGEN. cDNA was synthesized by GeneChip WT PLUS Reagent Kit (Thermo Fisher Scientific, MA, USA), then in vitro transcription, quantification, purification and reverse transcription of cRNA were performed. Next, the synthesis, purification, fragmentation and labeling of single-stranded cDNA were performed. Fragmented and labeled cRNA samples were hybridized using the cartridge array (Clariom S array, mouse; Thermo Fisher Scientific, MA, USA) on the GeneChip™ Fluidics Station and scanned by GeneChip Scanner (Thermo Fisher Scientific, MA, USA). Washing, staining, and scanning of the hybridized arrays were performed using GeneChip™ Hybridization, Wash and Stain Kit.

2.7. Microarray data processing and subsequent analyses

Raw image data processing and normalization was performed with Transcriptome Analysis Console (TAC) software version 4.0.2 (Thermo Fisher Scientific, MA, USA) following the signal space transformation robust multi-chip analysis (SST-RMA) algorithm, which background reduced via GC Correction Version 4. Then, the gene level analysis was performed using the Limma Bioconductor package in TAC software. Filter criteria for differentially expressed genes (DEGs) were set at p-value <0.05, and $-1.1 < \text{linear fold change} > 1.1$. DEGs were analyzed using the functional annotation tools of The Database for Annotation, Visualization and Integrated Discovery (DAVID) Knowledgebase [17] (<https://david.ncifcrf.gov/>. Accessed on May 2, 2022). A generic PPI network was constructed using an online tool NetworkAnalyst version 3.0 [18]. We built the first-order PPI network using the IMEx Interactome database comprised of Literature-curated comprehensive data from InnateDB [19]. Heatmaps were generated by the Morpheus online tool (<https://software.broadinstitute.org/morpheus>. Accessed on May 26, 2022). Gene-disease association was predicted by the Comparative Toxicogenomics Database (CTD) (<http://ctdbase.org/> Accessed on July 10, 2022). Transcription factor co-occurrence was checked by Enrichr (<https://maayanlab.cloud/Enrichr/> Accessed on November 5, 2022)

2.8. Scanning electron microscopy (SEM) imaging of SQ derivatives aggregations

SEM measurement was conducted on a Hitachi S-4300 field-emission scanning electron microscopy. The dried sample was subjected to SEM observation at an acceleration voltage of 1.0 kV.

2.9. Statistical analysis

Values were expressed as mean \pm SEM. GraphPad Prism 9.0 was used for data analysis and image processing. Differences between the groups were analyzed using ANOVA followed by Dunnett's posthoc test. P-values smaller than 0.05 were considered statistically significant.

3. Results

3.1. SQ and its EG derivatives induced different gene expression patterns during 3T3-L1 cell differentiation

Cell viability is one of the important indicators in the process of cell induction and differentiation. The cell viability rate of 3T3-L1 cells was evaluated by different doses of SQ and its EG derivatives for 24 h (Fig. 1b), and all compounds showed no significant cytotoxicity on 3T3-L1 cells until 80 μM of dose.

We separately examined the differentiation conditions of 3T3-L1 cells cultured after 7, 9, and 14 days; the cells reached full maturity by day 14 (Fig. S1). Furthermore, our study checked the impacts of SQ and its derivatives at 5 μM , 10 μM , and 20 μM doses. Given our objective to compare the effect across several derivatives, we kept the lowest dose for further analysis. Therefore, we selected 3T3-L1 cells treated with 5 μM of SQ and its derivatives for 14 days for microarray analysis.

Compared to the control group, genes with p-value <0.05, and $-1.1 < \text{linear fold change} > 1.1$ in all 22206 gene probe sets were identified as DEGs. Volcano plots showed up- and downregulated DEGs (Fig. 1c). Compared with the SQ-treated group, all derivatives promoted the expression of DEGs shown in the butterfly bar graph. The di-SQ and tri-SQ groups had comparable changes in the number of DEGs, and the tetra-SQ group had the highest number of DEGs (Fig. 1d). In tetra-SQ treated cells, 2144 genes were differentially expressed, among which 838 DEGs were upregulated and 1306 DEGs were downregulated.

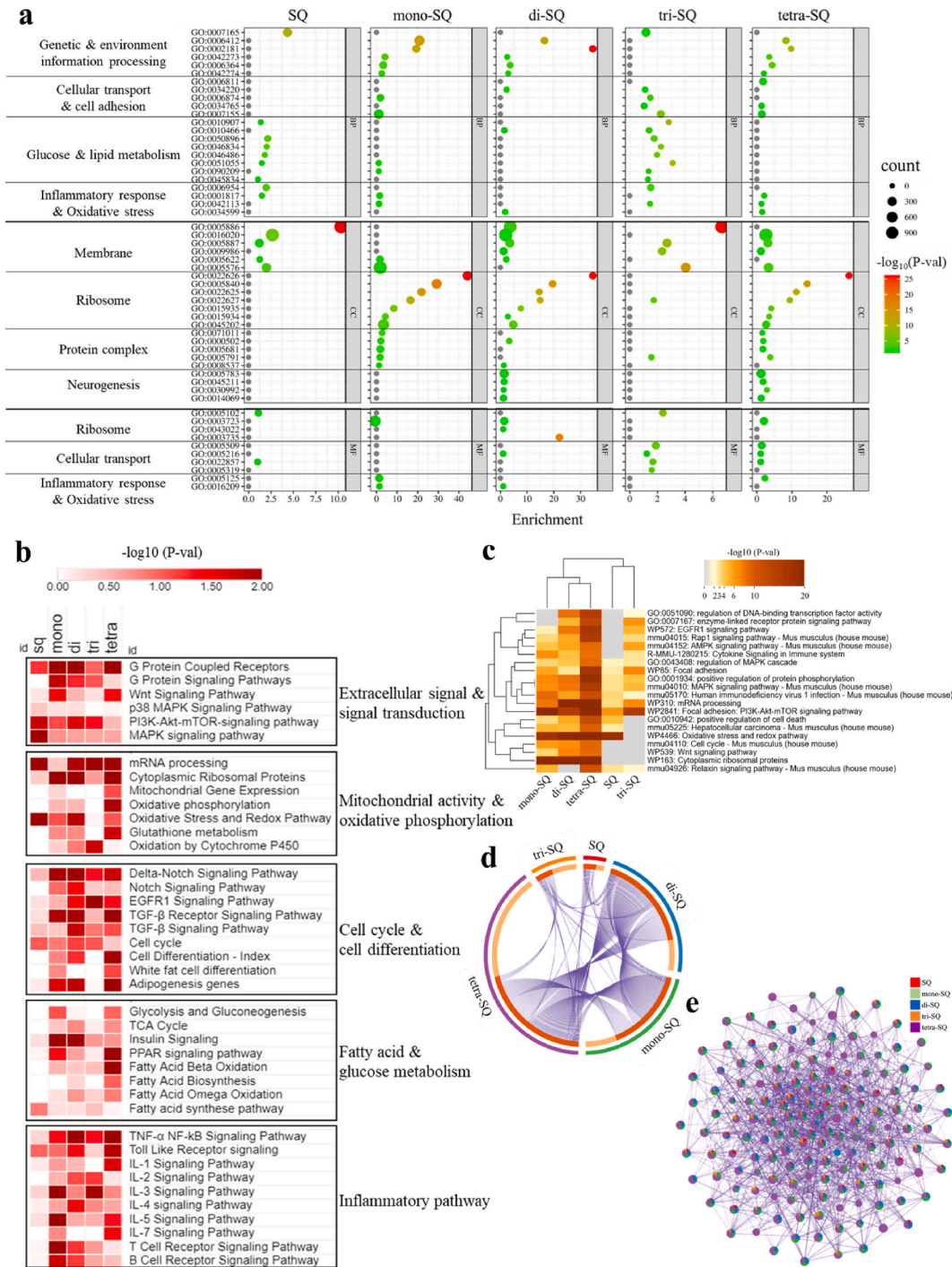


Fig. 2. Functional similarity of SQ and EG derivatives.

(a) GO analysis in SQ and its derivatives. Bubble plots showing the significance and enrichment of BP, CC and molecular functions (MF) in SQ and EG derivatives-treated cells compared to control cells. The size of the dot represents the count of gene expression in that term, color represents the p-value, dark grey dots for unexpressed GO term. (b) Heatmaps showing $-\log_{10}(P\text{-value})$ of WikiPathways. (c) Hierarchical cluster plot with statistically enriched terms using genes included in heatmap pathways. Statistically enriched terms accumulative hypergeometric p-values and enrichment factors were calculated and used for filtering by Metascape. Remaining significant terms were then hierarchically clustered into a tree based on Kappa-statistical similarities among their gene memberships. Then 0.3 kappa score was applied as the threshold to cast the tree into term clusters. (d) The Circos plot shows how genes from the heatmap gene list overlap. Each arc represents a gene list. The dark orange color represents shared genes, while the light orange color represents unique genes in SQ or EG derivatives. Purple lines link the same shared gene. (e) A PPI network was made using the above pathway gene list. Network nodes are displayed as pies. The color code for the pie sector represents a component.

3.2. SQ and its EG derivatives regulated a wide range of biological functions

We conducted gene ontology (GO) enrichment analyses to explore the biological functions of SQ and its derivatives. Significant GO biological processes and cellular components with a p-value <0.05 were selected.

In GO analysis, SQ and its derivatives showed different expression patterns. Terms related to glucose metabolism, lipid metabolism

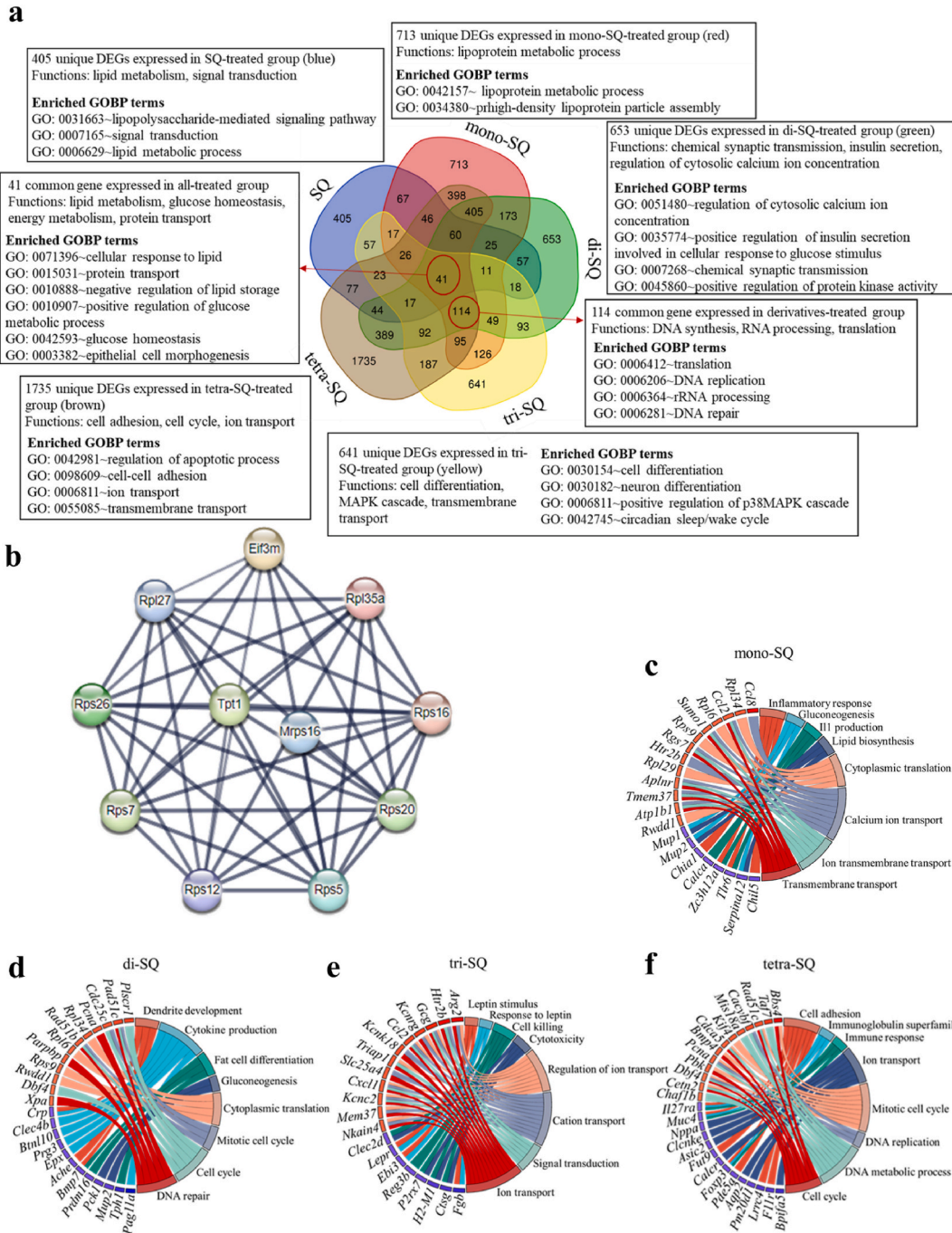


Fig. 3. Common and unique functions of EG derivatives.

(A)Venn diagram showing the number of common and unique DEGs of each group. (B) Predicted protein-protein interaction network of the 114 DEGs commonly enriched in all four derivatives, but not in squalene. Using chord plot to show the relationship between GO term and genes. (C) for mono-SQ, (D) for di-SQ, (E) for tri-SQ, (F) for tetra-SQ. Each color of clusters represents a GO term, color on the side of the gene represents the logFC of the gene, red represents up-regulation, blue represents down-regulation, and the darker the color, the larger the logFC value.

and membrane were significantly enriched in SQ. Mono-SQ can induce more GO term expressions related to cellular transport & cell adhesion, ribosome, protein complex and inflammatory response. Genes induced by di-SQ were enriched in cellular transport & cell adhesion, membrane, ribosome, neurogenesis and oxidative stress-related GO terms. Genes expressed in cells induced by tri-SQ showed a similar expression pattern to SQ and were enriched in the GO terms, including cellular transport, cell adhesion, glucose metabolism, lipid metabolism, inflammatory response and membrane. The tetra-SQ group had the highest count of enriched genes and covered all terms except glucose & lipid metabolism (Fig. 2a, Figs. S2a and b). These data suggested that both SQ and its derivatives can significantly enrich biological processes, cellular components and molecular functions, and EG derivatives showed better effects in ribosome and anti-inflammation.

3.3. SQ and its EG derivatives regulated signaling pathways during 3T3-L1 cell differentiation

We next examined the effects of SQ and its derivatives on signaling pathways during the induced differentiation of 3T3-L1 pre-adipocytes. We selected pathways related to adipose differentiation and lipid metabolism and then ranked them according to their biological process *in vivo*. SQ and its derivatives showed similar ability in regulating extracellular signal & signal transduction. All five components can enhance the mRNA process and cytoplasmic ribosome protein pathway, but in mitochondrial activity and oxidative phosphorylation-related pathways, mono-SQ, di-SQ and tetra-SQ showed more obvious enhancement. Similarly, cell cycle & cell differentiation are also strongly induced by mono-SQ, di-SQ, and tetra-SQ, not SQ or tri-SQ. All derivatives were associated with the

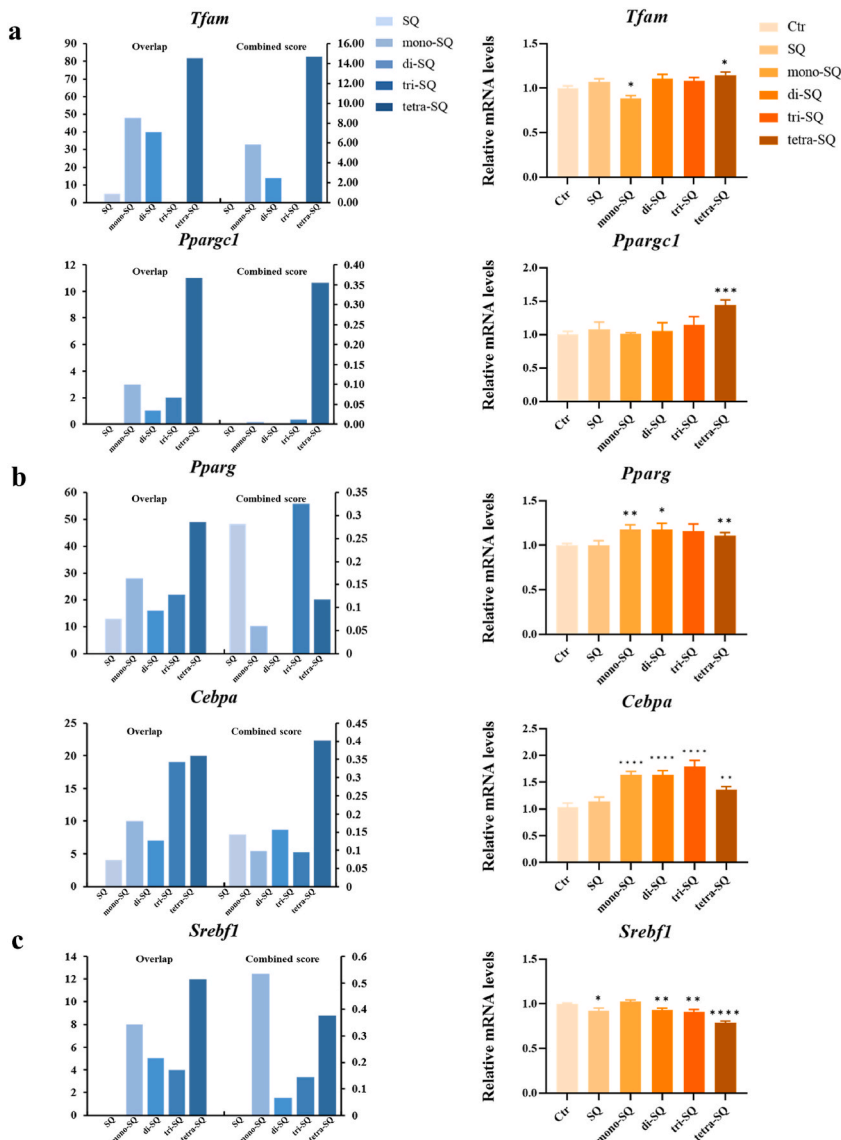


Fig. 4. Transcription factor activity.

enrichment of pathways involved in fatty acid and glucose metabolism, and the effect of tetra-SQ is the most obvious. Simultaneously inflammatory pathways were significantly enriched in all derivatives (Fig. 2b, Figs. S3a–d).

Since the biological processes involved in SQ and the four EG derivatives showed significant differences, we made a hierarchical clustering plot using the significantly enriched genes involved in Fig. 2B to check the similarity of SQ and the four derivatives' expression patterns. Through the clustering plot, we found di- and tetra-SQ had the highest similarity of expression patterns, followed by mono-SQ. SQ and tri-SQ had relatively close expression patterns (Fig 2c–e), and more than half of the genes of tetra- and tri-SQ were unique genes (Fig. 2d). The three most strongly expressed pathways were related to focal adhesion, oxidative stress, and cytoplasmic ribosome (Fig. 2c).

Therefore, further examination of overlapping genes' functions of the derivatives may help us intuitively understand the changes in the transcriptome.

3.4. Four EG derivatives showed similar functions in DNA and RNA processes

A Venn diagram of five components was created to explore further the similar functions between SQ and its derivatives and the unique role of each derivative. The five components share 41 common genes, which play a role mainly in regulating lipid storage and glucose metabolism (Fig. 3a); 4 derivatives shared 114 genes and were significantly enriched in DNA and RNA-related processes, in particular, large and small ribosomes were closely related in the predicted protein-protein interaction network (Fig. 3a and b). In addition, each component had unique genes and physiological roles. SQ was related to signal transduction and lipid metabolism, mono-SQ was related to lipoprotein, the most specific function of di-SQ was to regulate insulin secretion, tri-SQ regulated cell differentiation, genes in tetra-SQ-treated enhanced in transmembrane transport GO term (Fig. 3a). We also examined the relationship of genes in each derivative to pathways related to lipid metabolism or adipocyte differentiation by chord plots. All derivatives were associated with downregulated inflammatory pathways. Genes and pathways related to gluconeogenesis, lipid synthesis, and leptin were downregulated by mono-, di-, and tri-SQ, but not tetra-SQ. In addition, genes and pathways related to the inhibition of dendrite development were downregulated by di-SQ, while genes and pathways related to cell adhesion and ion transport were downregulated by tetra-SQ (Fig 3c–f). Among the upregulated pathways, di- and tetra-SQ were consistently associated with cell cycle and DNA metabolism and repair. Tri-SQ, like mono-SQ, was significantly related to signal transduction and ion transport (Fig 3c–f). Through parallel analysis of the four EG derivatives, we found that the expression patterns of di-SQ and tetra-SQ had the highest similarity, followed by mono-SQ, and tri-SQ had a unique expression pattern that was more similar to SQ. The common function of the four derivatives lies in the anti-inflammatory effect and regulation of DNA, RNA, and translation process.

3.5. Transcriptional factors of preadipocyte differentiation were markedly affected by EG derivatives of SQ

To verify the conclusions drawn by microarray at the gene level, we used the TF co-occurrence data set from Enrichr to detect the expression of transcription factors and used real-time PCR to verify the conclusions. Mitochondria not only regulate cellular energy homeostasis but are also strongly associated with adipose tissue, such as lipid metabolism, insulin sensitivity, and metabolic diseases [20]. Thus, we checked transcription factors related to mitochondrial biogenesis [21,22], transcription factor A, mitochondrial (*Tfam*) and peroxisome proliferator-activated receptor gamma (*Pparg*) coactivator 1 (*Ppargc1*) as transcription factors to check how derivatives influence mitochondrial function. Tetra-SQ has the largest DEG numbers in 2 transcription factors related to mitochondrial function, followed by mono. Tetra-SQ also has the highest combined score, which was calculated using z-score and p-value. The real-time PCR results also showed that compared with the control group, only tetra-SQ could significantly increase *Tfam* and *Ppargc1* expression levels, although SQ and its derivatives showed an overall upregulated tendency (Fig. 4a).

We then selected adipogenesis markers CCAAT enhancer binding protein alpha (*Cebpa*) and *Pparg* as TFs to validate the effect of SQ and its derivatives on adipogenesis. Similarly, tetra-SQ induced more overlap of genes associated with *Cebpa* and *Pparg*, followed by tri-SQ. And tri-SQ had the highest combined score in *Pparg*, while tetra-SQ had the highest combined score in *Cebpa*. As to Real Time-PCR results, all EG derivatives significantly enhanced the expression levels of *Cebpa* and *Pparg* compared to the control group, except tri-SQ in *Pparg* expression (Fig. 4b).

Unlike adipogenesis, lipogenesis is prone to obesity and diabetes [23]. Sterol regulatory element binding protein-1 (*Srebf1*) plays an important role in liver-induced lipogenesis, causing the accumulation of excess nutrients in the body [24]. According to the TF co-occurrence data set, tetra-SQ and mono-SQ accounted for the largest number of overlapped genes and combined scores, respectively. Compared with the control group, *Srebf1* expression levels in the EG derivative groups showed a downregulated tendency and had significance in di-, tri-, and tetra-SQ treated group (Fig. 4c).

Overall, we found that all EG derivatives can promote adipogenesis, and tetra-SQ treatment had a better effect in terms of improving mitochondrial function and alleviating lipid accumulation.

Effects of SQ and its derivatives on the expression of genes associated with (a) mitochondrial function, (b) Adipogenesis, (c) lipogenesis. Blue bar graphs (left) showing the number of overlapped DEGs and the combined scores of TF co-occurrence data set from microarray data. Orange bar graphs (right) showing mRNA expression in RT-qPCR.

3.6. Di- and tetra-SQ induced the generation of smaller LDs in adipocytes

Adipogenesis and lipid accumulation will be manifested as an increase in the number of LDs and an increase in the size of LDs, respectively. The size of LDs has a significant impact on adipocyte metabolism. Excess energy in the body is stored in LDs, and the

increase in LD size leads to pathological overgrowth of adipose tissue, such as inflammation, fibrosis, and insulin resistance [25,26].

Therefore, we also want to explore how SQ, and its derivatives could influence LD content and size in induced adipocytes. Compared with the control group, SQ and its derivatives could generate a larger number of LDs as found inORO staining images, especially tri- and tetra-SQ. However, compared to the control and SQ-treated groups, di- and tetra-SQ-treated groups showed smaller LDs (Fig. 5a). Then, we further examined the expression of genes associated with the formation of smaller LDs. The heatmap result showed the related genes in mono-, di-, and tetra-SQ were upregulated, in the SQ group were not expressed, and in the tri-SQ group were downregulated (Fig. 5b), which was consistent with the results in Fig. 5A. Furthermore, results of real-time PCR analysis showed that genes related to smaller LD formation, like eukaryotic translation initiation factor 4A3 (*Eif4a3*), were significantly upregulated by di- and tetra-SQ and were downregulated by SQ. The same trend was observed in TATA-box binding protein associated factor 9 (*Taf9*). However, the changes were not significant (Fig. 5c and d).

These results suggested that di- and tetra-SQ induced 3T3-L1 cells to generate large numbers and smaller-sized LDs during differentiation, which may improve inflammatory or metabolic diseases.

SQ and its derivatives modulated lipid droplet formation in 3T3-L1 cells lipid droplets with different phenotype. (a) Representative Oil Red O staining images at the D14 after the adipocyte induction. (b) Heatmap showing the expression pattern of DEGs in microarray that regulate lipid droplets size. mRNA expression of (c) *Eif4a3* and (d) *Taf9* in RT-qPCR in SQ and its derivatives treated cells.

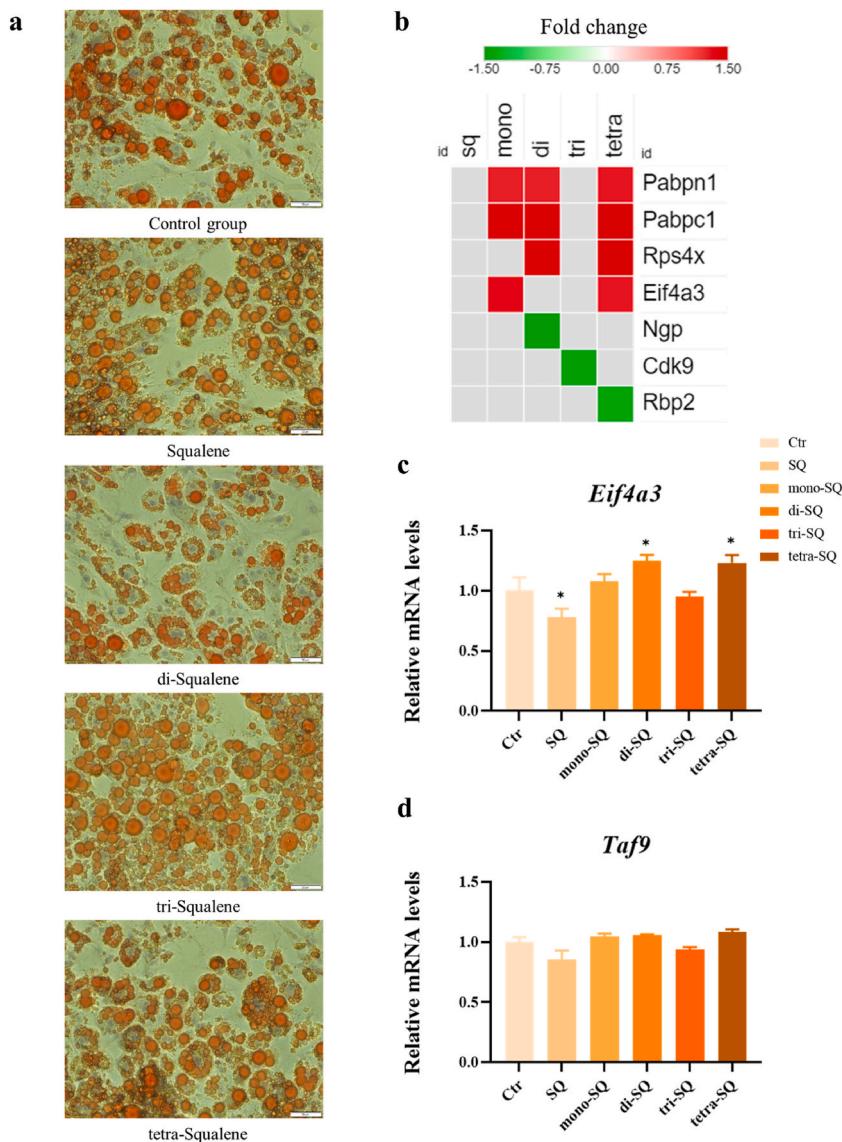


Fig. 5. Phenotypes of lipid droplet in SQ and EG derivatives.

3.7. EG derivatives ameliorated cellular inflammation and metabolic diseases

We investigated the effects of SQ and its EG derivatives on inflammatory responses and metabolic diseases during adipogenesis.

According to the cytokines data in the microarray analysis, SQ and its derivatives could downregulate the expression of most inflammatory cytokine genes, and 50 cytokine genes were downregulated by tetra-SQ. In all 80 adipokines from microarray data, SQ and its derivatives prevented the overexpression of a large number of inflammatory cytokines (Fig. 6a and b). Compared to the control group, all four EG derivatives can downregulate tumor necrosis factor (*Tnf*) expression level (Fig. 6c).

A specific adipose cytokine gene, adiponectin (*Adipoq*), which is involved in glucose regulation and reduces the risk of type 2 diabetes, was detected [27,28]. *Adipoq* was significantly increased in the di- and tetra-SQ treated groups and slightly increased in the mono-SQ treated group, although there was no statistical significance (Fig. 6d).

We next performed gene-disease association analysis to predict the effects of SQ and EG derivatives on human health. We mainly targeted metabolic and immune system-related diseases. We found that SQ and EG derivatives were associated with fibrosis, liver cirrhosis, nutritional and metabolic diseases, etc. Genes related to liver cirrhosis and fibrosis were downregulated in SQ and tri-SQ treated groups. However, genes related to immune system diseases were upregulated in the SQ-treated group and downregulated in the tri-SQ-treated group. Genes associated with the immune system, cirrhosis and nutrition and metabolism-related diseases were equally upregulated and downregulated in mono-, di-, and tetra-SQ treated groups. Specifically, di- and tetra-SQ can downregulate genes related to diabetes and glucose metabolism disorders, which may be associated with the formation of smaller LDs (Fig. 7a).

To verify these results, disease-associated genes were further tested on RT-qPCR. Sirtuin 3 (*Sirt3*) has a close relationship with the regulation of adipogenesis and adipokine secretion, which may be a potential target for the improvement of type 2 diabetes [29].

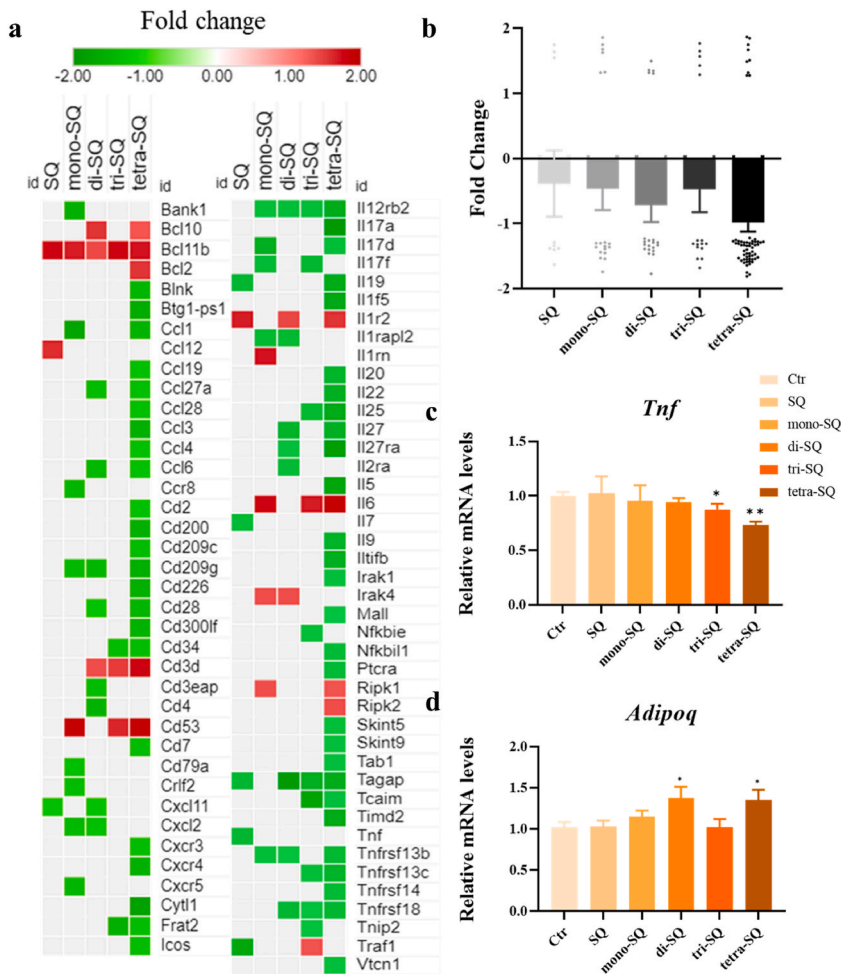


Fig. 6. Down- and upregulated cytokines.

SQ and derivatives inhibited the expressions of inflammatory cytokines in 3T3-L1 cells after D14 adipocyte differentiation. (a) Heatmap showing the expression pattern of significantly regulated proinflammatory cytokines (n = 80) in microarray. (b) Median average of fold changes of inflammatory cytokine selected from microarray data. (c) Relative gene expression of *Tnf* and (d) *Adipoq*, normalized to *Gapdh* as endogenous control, treated with 5 μM SQ and its derivatives until D14.

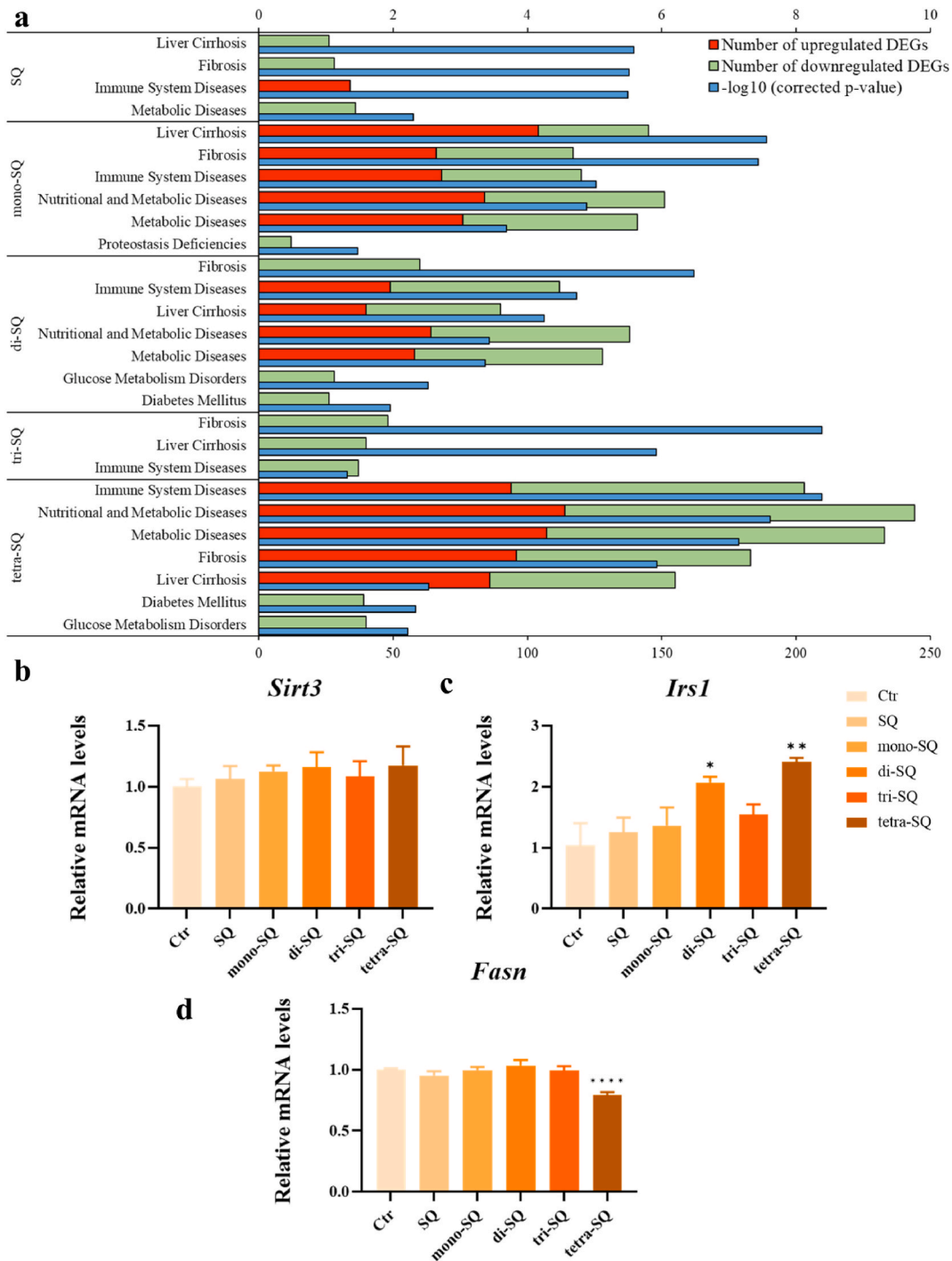


Fig. 7. Down- and upregulated metabolic disease and related gene. (a) Bar graph displaying the metabolic diseases that are statistically enriched among DEGs of SQ and its derivatives. Blue bars represent the significance of enrichment, and red bars represent the number of upregulated DEGs. Green bars represent the number of downregulated DEGs. The significance of enrichment is calculated by the hypergeometric distribution and adjusted for multiple testing using the Bonferroni method. Expression of genes (b) *Irs1*, (c) *Sirt3* and (d) *Fasn* in RT-qPCR.

Compared with the control group, both SQ and its EG derivatives treated groups showed an upregulation trend (Fig. 7b), although not with statistical significance. Insulin receptor substrate 1 (*Irs1*) signaling regulates glucose homeostasis [30] and improves insulin resistance [31]. After the induction of SQ and its EG derivatives, the expression level of *Irs1* showed an overall upregulation trend, especially di- and tetra-SQ showed statistical significance (Fig. 7c). As a downstream gene of *Srebf1*, fatty acid synthase (*Fasn*) is also

associated with excessive lipid accumulation. Increased *Fasn* gene expression exacerbates impaired insulin sensitivity and is associated with the development of type 2 diabetes [32], nonalcoholic fatty liver disease, and liver fibrosis [33]. Although genes related to fibrosis and liver cirrhosis in both SQ and its EG derivatives were downregulated, and genes related to diabetes were downregulated in both di-



and tetra-SQ in Fig. 7A, *Fasn* was only significantly downregulated by tetra-SQ treatment (Fig. 7d).

3.8. EG derivatives of SQ (mono-SQ, di-SQ, tri-SQ, tetra-SQ) self-organized into vesicles in pure water

SQ is completely insoluble in polar solvents (water, DMSO, alcohols, etc.), which precludes its facile administration to living organisms, and it is also unclear how it forms molecular aggregates in a so-called polar cellular environment. In this study, we found for the first time that the introduction of EG to SQ makes it soluble in polar solvents and forms large vesicles in water.

As shown in Fig. 8a of SEM images, the EG derivatives of SQ are self-organized into different vesicles in pure water. It was found that the shape and size of the vesicles changed when only the length of EG moiety was just varied. As for the SEM figures, the length error is about 20 %. That is, mono-SQ self-organized into one type of vesicle: rod oval-shaped vesicles: a length of 2.4 μm and diameter width of 0.39 μm ; di-SQ did two types of vesicles: rod oval-shaped vesicles: length of 2.9 μm and diameter width of 0.50 μm ; spherical vesicles: diameter of 0.44 μm ; tri-SQ did one type of vesicle: spherical vesicles: diameter of 0.35 μm ; and tetra-SQ did one type of vesicle: spherical vesicles: diameter of 0.44 μm , respectively, in pure water.

We have already shown that the 440 nm diameter spherical vesicles of tetra-SQ are sensitive to the surrounding polar environment and shrink to about 100 nm diameter spherical vesicles in the presence of alkaline earth metal cations [16]. Thus, it is suggested that the shape of the self-assembled form of EG derivatives of SQ is highly dependent on the polar environment around the cell.

3.9. Cation-binding activity revealed the effects of EG derivatives on immune responses and other observed functional differences

We built PPI networks to explore whether the cation-binding activity of the SQ derivatives was responsible for the differences observed in functional analyses.

In SQ and all derivatives, the top hub gene (with the highest degree) was the same for both 'undirected' and 'Cation Binding' PPI enrichment. Therefore, it can be assumed that the cation-binding activity of the derivatives is, in part, responsible for the transcriptional regulation (Fig. S4). The first-order network directed for 'cation binding' molecular function identified different hub genes in SQ and its derivatives (Fig. 8b, Fig. S4, Table S1). In SQ, *Nfe2* is the top hub node with the highest degree (degree = 31, betweenness = 6776.75, Fold change = -1.81). The top upregulated hub node in SQ is *Sumo1* (degree = 13, betweenness = 3288.19, Fold change = 2.02). All the EG derivatives had the common top hub node (forkhead box P3) *Foxp3*; however, its degree of interaction and expression varied among the derivatives. *Foxp3* in mono-SQ expressed as degree = 61, betweenness = 20019.73, Fold change = -1.8, in di-SQ expressed as degree = 61, betweenness = 16092.83, Fold change = -2.22, in tri-SQ expressed as degree = 59, betweenness = 14222.92, Fold change = -1.78, while in tetra-SQ, *Foxp3* expressed as degree = 68, betweenness = 22886.19, Fold change = -2.05.

Several cation-binding associated hub nodes were responsible for transcriptional regulation (Fig. 8c). The top 10 cation binding hub genes of SQ and its EG derivatives were selected to analyze top functions. In SQ, the hub gene *Nfe2* showed similar interaction (number of degrees) in mono-SQ but not in the other three EG derivatives. This result illustrates the similarity between SQ and mono on the cation-binding hub genes, but not the others. Compared to SQ, all EG derivatives showed ten times higher interaction with hub gene *Foxp3*, which plays an important role in immune tolerance [34], and showed the most obvious downregulation in di- and tetra-SQ treatment groups (fold change = -2.22, -2.05 respectively), and the highest interaction in tetra-SQ treatment groups (number of degrees = 68).

In addition, we also detected the KEGG pathways involved in the negative and positive regulation of transcription separately. In negative regulation of transcription, except di-SQ was related to ribosome and cell cycle, tetra-SQ was related to cell cycle and endocrine resistance, and all other top pathways in SQ and 4 EG derivatives were related to inflammatory response and immune response. While in positive regulation of transcription, inflammatory response and immune response-related pathways expressed in SQ and 4 EG derivatives. Ribosome and RNA processes-related pathways were upregulated by SQ and three derivatives except for tri-SQ. Metabolic process-related pathways were upregulated by di- and tetra-SQ, especially tetra-SQ, which was involved in the expression of the highest number of genes in these pathways (Fig. 8d). These results may reveal the reason why SQ-EG derivatives improved anti-inflammatory function.

Since alkaline earth metal cations can shrink the 440 nm diameter spherical vesicles of tetra-SQ to about 100 nm in diameter [16], we examined the enriched cation binding in SQ and its derivatives. Zinc ion binding (Table S2) was the top ion enriched in SQ and its derivatives, but the number of hits varied (SQ = 94, Mono = 154, Di = 111, Tri = 126, Tetra = 161). While copper ion binding (Table S2) was also enriched; however, the number of hits was considerably low (SQ = 3, Mono = 4, Di = 3, Tri = 6, Tetra = 5).

4. Discussion

This study confirmed that the insertion of EG moiety improved the biological activity of SQ in vitro, but also changed the structure and function. The study showed that when the length of the EG moiety in the derivative was altered, the shape and size of the vesicles were also changed. Therefore, the four derivatives have unique vesicle morphology or size, among which di- and tetra-SQ can form spherical vesicles with the same diameter of 0.44 μm , which may explain why the two derivatives have the most similar functions, especially in improving anti-inflammatory and glucose metabolism-related functions.

3T3-L1 cells exhibit fibroblast morphology and serve as preadipocytes, possessing the potential for directed differentiation. They are often used as a model for in vitro adipocyte research [35] and have found extensive utility in studies related to obesity [36], diabetes, and insulin resistance [37,38].

Microarray is a genomics research tool that can simultaneously detect the expression of thousands of genes [39] and has been

widely used in recent years.

Early adipocytes are plastic and can proliferate through hyperplasia or hypertrophy [40]. Hypertrophy increases the weight of adipose tissue and affects the release of adipokines [41], which may lead to proinflammatory features of obesity and increase the incidence of metabolic diseases such as type 2 diabetes and insulin resistance [42]. Preadipocyte hyperplasia can increase the overall volume of adipocytes while ameliorating the development of metabolic diseases [43]. To alleviate inflammation and metabolic diseases caused by the adipogenesis process, various natural substances have been shown to regulate preadipocytes during differentiation [15,44,45].

SQ and its derivatives are amphiphilic compounds synthesized by adding different amounts of mono EG to SQ [14], and do not affect the survival rate of 3T3-L1 preadipocytes. At the same time, the treatment of sq and its derivatives significantly altered the overall microarray expression pattern. Different derivatives have different effects on up- and downregulated genes and pathways. di- and tetra-, SQ and tri- showed higher Expression pattern similarity. The effects of the four derivatives are obviously unique; for example, tri-SQ is closely related to the transport pathway, while di- and tetra-SQ work in neurogenic pathways. The four derivatives showed similar effects only in the regulation of ribosome and DNA, RNA processing.

Among the pathways and GO terms, mitochondrial function and MAPK pathway are also regulated by four derivatives in varying degrees. Mitochondria play an important role in the maintenance of energy homeostasis in adipose tissue [46], and are related to specific functions such as lipogenesis, glucose metabolism, and insulin sensitivity [47–49]. After 14 days of differentiation, mono-, di- and tetra-SQ all enhanced mitochondrial activity and MAPK pathway significantly compared to the control group. And the inductive treatment of four derivatives was involved in the regulation of transcription factors and genes related to mitochondrial activity, adipogenesis and lipogenesis. In particular, tetra-SQ significantly upregulated the mitochondrial activity gene marker *Ppargc1* and *Tfam*, the early adipogenesis markers *Pparg* and *Cebpa*, and inhibit the overexpression of *Fasn* and *Srebfl* to reduce excessive lipid accumulation.

Lipogenesis was inhibited after 14 days of treatment with SQ and its derivatives, which caused changes in the size of LDs within the lipid cells. The effect of the derivatives on the size of LDs was significantly different, and di- and tetra-SQ had a significant effect on reducing LDs size. LDs size may be associated with insulin sensitivity and adipocyte inflammation but not total intracellular lipid content, just like in skeletal muscle [50,51].

Sirt3 has been proven to activate mitochondrial function and promote adaptive thermogenesis in brown adipose tissue [52] and showed an upward trend after 14 days of induction by SQ and its derivatives, although there is no significance. *Irs1* promotes adipocyte differentiation by upregulating the expression of *Cebpa* and *Pparg* [53] and is downregulated by obesity [54]. Our results showed di- and tetra-SQ can significantly upregulate the mRNA expression level of *Irs1*, which is consistent with disease prediction results; only di- and tetra-SQ can improve diabetes mellitus and glucose metabolism disorders. Although other derivatives also have the function of modulating metabolic diseases, di- and tetra-SQ undoubtedly have unique effects. This suggests that both SQ and its derivatives had positive effects in improving metabolism, and derivatives showed better effects.

The adipogenesis process is involved in the regulation of cytokines, such as TNF and IL-1, in adipose tissue [55]. Lipid accumulation causes the recruitment and activation of macrophages in adipose tissue, further aggravating the intracellular inflammatory response and increasing the risk of insulin resistance and type 2 diabetes [56,57]. All SQ derivatives can downregulate the expression of cytokines represented by *Tnf* in 3T3-L1 cells, especially tri- and tetra-SQ have significance. This shows that SQ derivatives have better anti-inflammatory effects, which may be related to changes in intracellular lipid droplet phenotype [43], thereby altering the production of proinflammatory factors and other mediator factors in adipocytes [58]. The gene expression levels of inflammatory cytokines ($n = 80$) (Table S3) from microarray data were downregulated under the regulation of SQ derivatives and were related to various inflammatory pathways. Compared with SQ, derivatives showed better effects in improving overall inflammatory status. This result is consistent with the anti-inflammatory effect of SQ amphiphilic derivatives in adipocytes from human adipose-derived stem cells [15], and murine macrophage-like cells [14].

EG derivatives of SQ dynamically self-organize into the vesicles in water according to the length of EG, and they can change the shape of the vesicles according to the polar environment. Depending on their respective cellular environments, such as the lipid differentiation process, EG derivatives may self-organize into a variety of different vesicles and express specific functions. The shape and size of self-assembled vesicles are known to be closely related to their physiologically active performance [59]. Therefore, it is necessary to clarify the self-assembled shape of EG derivatives in each cellular environment. Both di- and tetra-SQ can form a 0.44- μm -diameter spherical vesicle. According to our previous studies, vesicles at 0.44- μm -diameter are most susceptible to alkaline earth metal ions [16]. Under the influence of zinc and copper ions, the vesicles shrink and reduce in diameter to 0.1 μm , which may affect how they enter the cell [59]. Although tri-SQ can also form spherical vesicles, the difference in cation binding activities may explain the functional differences of tri-SQ observed in enrichment analyses.

The difference in cation binding activities also led to the difference in hub genes in the PPI network of SQ and its EG derivatives. The hub genes appeared in the PPI network of SQ and its four derivatives were all related to immune response or metabolic process. The reduction of nuclear factor erythroid 2-related factor 2 (*Nfe2*) expression has been proved to inhibit the expression of *Pparg* [60] and *Cebpa* [61], associated with adipocyte differentiation, obesity, and insulin resistance [62] and promote the tendency to develop autoimmune disorders [63]. According to our results, *Nfe2* expression was downregulated only in SQ and mono-SQ with similar interaction (number of degrees), but not in the other three EG derivatives; this may be related to the different self-organized vesicles of mono-SQ. *Foxp3* protects from lipotoxicity by driving oxidative phosphorylation [64] and is a specific marker of naive T regulatory cells [65], which is closely related to self-tolerance and autoimmune responses [66]. Interestingly, *Foxp3* was significantly downregulated in all four EG derivatives but was not affected by SQ. Meanwhile, the highest fold change and highest interaction of *Foxp3* were observed in di- and tetra-SQ, which formed spherical vesicles of the same diameter in pure water. This substantiated that the

addition of the EG moiety improves the immune function of derivatives, especially autoimmunity. Further, it seems that spherical vesicles with larger diameters work better. These results may reveal the reason why EG derivatives improved anti-inflammatory function. Nevertheless, the correlation between the structure of EG derivatives and their functionality within the cellular environment is yet to be fully elucidated. Furthermore, the impact of the biological activity of EG derivatives within an *in vivo* setting requires additional exploration.

In summary, although the SQ derivatives improved the hydrophilicity of SQ, they showed apparent differences in the process of lipid differentiation. Especially tri-SQ was similar to SQ in almost all functions in the genetic and environmental information process (e.g., ribosome biogenesis, protein stabilization). This may be related to the difference in the 3D structure of tri-SQ and other derivatives; tri-SQ has a smaller structure, so perhaps it has a different way of exogenous substances entering cells from other derivatives. In addition, di- and tetra-SQ showed high concordance in lipid droplet size (e.g., *Eif4a3* and *Taf9* mRNA expression level) and lipid metabolism (e.g., insulin signaling pathway and PPAR signaling pathway), especially regulation of glucose metabolism and insulin secretion, which were distinctly different from other derivatives. Both di- and tetra-SQ self-organized into similar sizes and shapes of vesicles, which subsequently improved their cation binding activities. This suggests that spherical vesicles with larger diameters can better improve metabolic function and immune effect. Protein-protein interaction networks further revealed that cation binding activity might explain a major part, if not all, of the differences observed in functional analyses.

5. Conclusion

The results of this experiment showed that both SQ and its derivatives can promote the adipogenesis of 3T3-L1 cells and ameliorate inflammatory response (Fig. 9). Tri-SQ has a high similarity to SQ, specifically enhancing signal transduction and transmembrane transport. Di- and tetra-SQ have the highest similarity, which is manifested in the self-organized vesicles' sizes, shapes, and functions. They inhibited the excessive accumulation of lipid during the process of adipogenesis and alleviated metabolic disorders and insulin resistance caused by obesity and other metabolic-related diseases. The research could help to promote the development of natural compound replacement therapy and provide adjunct therapy to improve obesity and diabetes-related conditions.

Funding

This work was supported by the Japan Science and Technology Agency (JST grant number JPMJPF2017) and Japan Science and Technology-OPERA program (JPMJOP 1832). The funders had no role in the design of the study; in the collection, analyses, or interpretation of data; in the writing of the manuscript; or in the decision to publish the results.

Availability of data and materials

The supporting data of this article can be found within this paper. The microarray data have been deposited in the NCBI GEO database and are publicly available (GSE224049 <https://www.ncbi.nlm.nih.gov/geo/query/acc.cgi?acc=GSE224049>).

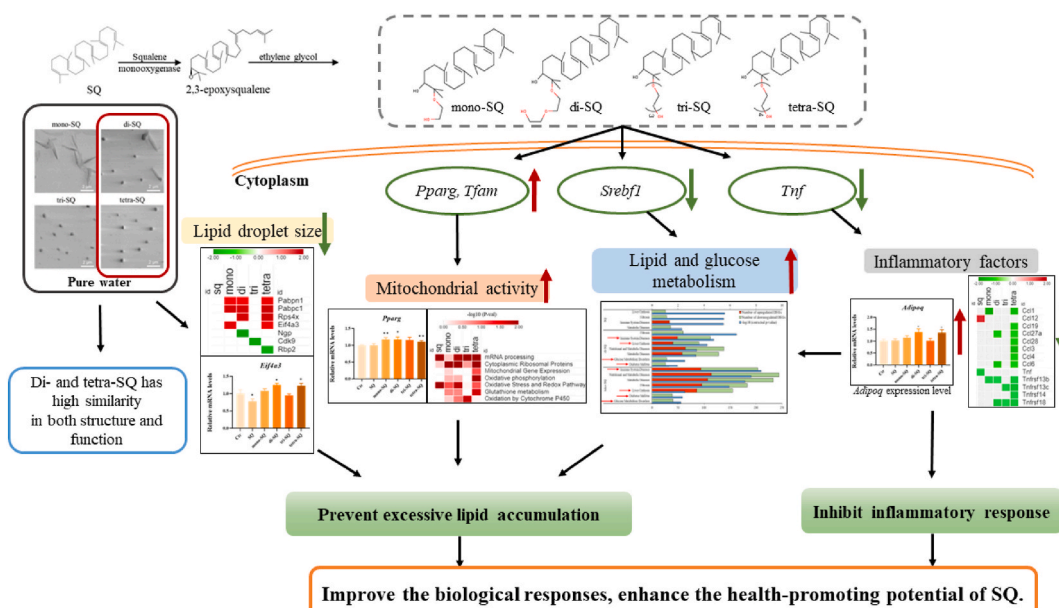


Fig. 9. Summary of SQ EG derivatives' functions.

Ethics approval and consent to participate

Not applicable.

Consent for publication

All the authors approved the final version of the article.

CRediT authorship contribution statement

Yu Cheng: Methodology, Software, Validation, Visualization, Writing – original draft, Writing – review & editing, Conceptualization. **Farhana Ferdousi:** Methodology, Conceptualization, Software, Visualization, Writing – review & editing. **Bryan Angelo Foronda:** Methodology. **Tran Ngoc Linh:** Visualization, Writing – original draft, Writing – review & editing. **Munkhzul Ganbold:** Methodology. **Akira Yada:** Resources, Writing – review & editing. **Takashi Arimura:** Conceptualization, Resources, Visualization, Writing – review & editing. **Hiroko Isoda:** Conceptualization, Funding acquisition, Project administration, Resources, Supervision, Writing – review & editing.

Declaration of competing interest

The authors declare that they have no known competing financial interests or personal relationships that could have appeared to influence the work reported in this paper.

Abbreviations

cDNA	Complementary DNA
CTD	Comparative Toxicogenomics Database
DAVID	Database for Annotation, Visualization and Integrated Discovery
DEG	Different Expressed Gene
DMSO	Dimethyl sulfoxide
EG	Ethylene Glycol
GO	Gene Ontology
LD	Lipid Droplet
MF	molecular functions
MTT	3-(4,5-Dimethylthiazol-2-yl)-2,5-diphenyltetrazolium bromide
Nfe2	Nuclear factor erythroid 2-related factor 2
PPI	Protein-Protein Interaction
SEM	Scanning Electron Microscopy
SQ	Squalene
TAC	Transcriptome Analysis Console
Tregs	T regulatory cells

Appendix A. Supplementary data

Supplementary data to this article can be found online at <https://doi.org/10.1016/j.heliyon.2024.e26867>.

References

- [1] M. Hernández-Pérez, et al., Squalene content in livers from deep-sea sharks caught in Canary Island waters, *Mar. Freshw. Res.* 48 (7) (1997) 573–576.
- [2] H.-P. He, H. Corke, Oil and squalene in amaranthus grain and leaf, *J. Agric. Food Chem.* 51 (27) (2003) 7913–7920.
- [3] C. Cabrera-Vique, et al., Bioactive compounds and nutritional significance of virgin argan oil—an edible oil with potential as a functional food, *Nutr. Rev.* 70 (5) (2012) 266–279.
- [4] N. Shimizu, et al., Significance of squalene in rice bran oil and perspectives on squalene oxidation, *J. Nutr. Sci. Vitaminol.* 65 (Supplement) (2019) S62–S66.
- [5] K. Kaya, et al., Thraustochytrid *Aurantiochytrium* sp. 18W-13a accumulates high amounts of squalene, *Biosc. Biotech. Biochem.* 75 (11) (2011) 2246–2248.
- [6] K.E. Bloch, Sterol, structure and membrane function, *Crit. Rev. Biochem.* 14 (1) (1983) 47–92.
- [7] C.V. Rao, H.L. Newmark, B.S. Reddy, Chemopreventive effect of squalene on colon cancer, *Carcinogenesis* 19 (2) (1998) 287–290.
- [8] F.E. Güneş, Medical use of squalene as a natural antioxidant, *Journal of Marmara University Institute of Health Sciences* 3 (4) (2013).
- [9] A. Cárdeno, et al., Squalene targets pro-and anti-inflammatory mediators and pathways to modulate over-activation of neutrophils, monocytes and macrophages, *J. Funct. Foods* 14 (2015) 779–790.
- [10] N.I. Ibrahim, et al., The efficacy of squalene in cardiovascular disease risk—a systematic review, *Nutrients* 12 (2) (2020) 414.
- [11] T.E. Strandberg, R.S. T. T.A. Miettinen, Metabolic variables of cholesterol during squalene feeding in humans: comparison with cholestyramine treatment, *J. Lipid Res.* 31 (1990) 1637–1643.
- [12] J.S. Suk, et al., PEGylation as a strategy for improving nanoparticle-based drug and gene delivery, *Adv. Drug Deliv. Rev.* 99 (2016) 28–51.

- [13] S.N. Alconcel, A.S. Baas, H.D. Maynard, FDA-approved poly (ethylene glycol)–protein conjugate drugs, *Polym. Chem.* 2 (7) (2011) 1442–1448.
- [14] K. Sasaki, et al., Synthesis of 2-(2-Hydroxyethoxy)-3-hydroxysqualene and characterization of its anti-inflammatory effects, *BioMed Res. Int.* (2020) 2020.
- [15] M. Ganbold, et al., New amphiphilic squalene derivative improves metabolism of adipocytes differentiated from diabetic adipose-derived stem cells and prevents excessive lipogenesis, *Front. Cell Dev. Biol.* 8 (2020) 577259.
- [16] T.N. Linh, et al., Syntheses and aggregation properties of new squalene receptors bearing open chain ligands, *Supramol. Chem.* 33 (5) (2021) 194–201.
- [17] D.W. Huang, et al., DAVID Bioinformatics Resources: expanded annotation database and novel algorithms to better extract biology from large gene lists, *Nucleic Acids Res.* 35 (suppl_2) (2007) W169–W175.
- [18] J. Xia, M.J. Benner, R.E. Hancock, NetworkAnalyst-integrative approaches for protein–protein interaction network analysis and visual exploration, *Nucleic Acids Res.* 42 (W1) (2014) W167–W174.
- [19] K. Breuer, et al., InnateDB: systems biology of innate immunity and beyond—recent updates and continuing curation, *Nucleic Acids Res.* 41 (D1) (2013) D1228–D1233.
- [20] J.H. Lee, et al., The role of adipose tissue mitochondria: regulation of mitochondrial function for the treatment of metabolic diseases, *Int. J. Mol. Sci.* 20 (19) (2019) 4924.
- [21] W.-F.L.N.S. Chouinard, M. Lazar, P.C. Chui, J. Leszyk, J. Straubhaar, M.P. Czech, S. Corvera, Mitochondrial remodeling in adipose tissue associated with obesity and treatment with rosiglitazone, *J. Clin. Invest.* 114 (2004) 1281–1289.
- [22] A. De Pauw, et al., Mitochondrial (dys) function in adipocyte (de) differentiation and systemic metabolic alterations, *Am. J. Pathol.* 175 (3) (2009) 927–939.
- [23] P.A. Lewandowski, et al., The role of lipogenesis in the development of obesity and diabetes in Israeli sand rats (*Psammomys obesus*), *J. Nutr.* 128 (11) (1998) 1984–1988.
- [24] S. Li, M.S. Brown, J.L. Goldstein, Bifurcation of insulin signaling pathway in rat liver: mTORC1 required for stimulation of lipogenesis, but not inhibition of gluconeogenesis, *Proc. Natl. Acad. Sci. USA* 107 (8) (2010) 3441–3446.
- [25] K. Sun, C. Kusminski, Ph Scherer, Adipose tissue remodeling and obesity, *J. Clin. Invest.* 121 (2011) 2094–2101.
- [26] M. Konige, H. Wang, C. Sztalryd, Role of adipose specific lipid droplet proteins in maintaining whole body energy homeostasis, *Biochim. Biophys. Acta, Mol. Basis Dis.* 1842 (3) (2014) 393–401.
- [27] K. Ghoshal, et al., Adiponectin genetic variant and expression coupled with lipid peroxidation reveal new signatures in diabetic dyslipidemia, *Biochem. Genet.* 59 (3) (2021) 781–798.
- [28] L. Forný-Germano, F.G. De Felice, M.N.d.N. Vieira, The role of leptin and adiponectin in obesity-associated cognitive decline and Alzheimer's disease, *Front. Neurosci.* 12 (2019) 1027.
- [29] O. Ma, et al., Sirt3 regulates adipogenesis and adipokine secretion via its enzymatic activity, *Pharmacology Research & Perspectives* 8 (6) (2020) e00670.
- [30] X. Dong, et al., Irs1 and Irs2 signaling is essential for hepatic glucose homeostasis and systemic growth, *J. Clin. Invest.* 116 (1) (2006) 101–114.
- [31] Y. Wang, P.M. Nishina, J.K. Naggert, Degradation of IRS1 leads to impaired glucose uptake in adipose tissue of the type 2 diabetes mouse model TALLYHO/Jng, *J. Endocrinol.* 203 (1) (2009) 65.
- [32] J. Berndt, et al., Fatty acid synthase gene expression in human adipose tissue: association with obesity and type 2 diabetes, *Diabetologia* 50 (2007) 1472–1480.
- [33] C. Dorn, et al., Expression of fatty acid synthase in nonalcoholic fatty liver disease, *Int. J. Clin. Exp. Pathol.* 3 (5) (2010) 505.
- [34] J.D. Fontenot, M.A. Gavin, A.Y. Rudenski, Foxp3 programs the development and function of CD4+ CD25+ regulatory T cells, *Nat. Immunol.* 4 (4) (2003) 330–336.
- [35] H.-L. Kim, et al., Anti-obesity effects of a mixture of atractylodes macrocephala and amomum villosum extracts on 3T3-L1 adipocytes and high-fat diet-induced obesity in mice, *Molecules* 27 (3) (2022) 906.
- [36] M. Malodobra-Mazur, A. Cierznia, T. Dobosz, Oleic acid influences the adipogenesis of 3T3-L1 cells via DNA Methylation and may predispose to obesity and obesity-related disorders, *Lipids Health Dis.* 18 (1) (2019) 1–15.
- [37] M. Thomson, M.G. Williams, S.C. Frost, Development of insulin resistance in 3T3-L1 adipocytes, *J. Biol. Chem.* 272 (1997) 7759–7764.
- [38] B. Etesami, et al., Investigation of 3T3-L1 cell differentiation to adipocyte, affected by aqueous seed extract of Phoenix Dactylifera L, *Reports of Biochemistry & Molecular Biology* 9 (1) (2020) 14.
- [39] E. Glaab, J.M. Garibaldi, N. Krasnogor, ArrayMining: a modular web-application for microarray analysis combining ensemble and consensus methods with cross-study normalization, *BMC Bioinf.* 10 (1) (2009) 1–7.
- [40] J. Jo, et al., Hypertrophy and/or hyperplasia: dynamics of adipose tissue growth, *PLoS Comput. Biol.* 5 (3) (2009) e1000324.
- [41] T. Skurk, C. Bertl-Huber, C. Herder, H. Hauner, Relationship between adipocyte size and adipokine expression and secretion, *J. Clin. Endocrinol. Metab.* 92 (2007) 1023–1033.
- [42] S.E. Kahn, R.L. Hull, K.M. Utzschneider, Mechanisms linking obesity to insulin resistance and type 2 diabetes, *Nature* 444 (7121) (2006) 840–846.
- [43] A.L. Ghaben, P.E. Scherer, Adipogenesis and metabolic health, *Nat. Rev. Mol. Cell Biol.* 20 (4) (2019) 242–258.
- [44] L.-Y. Wu, et al., Curcumin attenuates adipogenesis by inducing preadipocyte apoptosis and inhibiting adipocyte differentiation, *Nutrients* 11 (10) (2019) 2307.
- [45] T. Li, et al., Pomegranate flower extract bidirectionally regulates the proliferation, differentiation and apoptosis of 3T3-L1 cells through regulation of PPAR γ expression mediated by PI3K-AKT signaling pathway, *Biomed. Pharmacother.* 131 (2020) 110769.
- [46] D.L. Johannsen, E. Ravussin, The role of mitochondria in health and disease, *Curr. Opin. Pharmacol.* 9 (6) (2009) 780–786.
- [47] F. Gregoire, C.M. Smas, H.S. Sul, Understanding adipocyte differentiation, *Physiol. Rev.* 78 (1998) 783–809.
- [48] C. Vernochet, et al., Adipose tissue mitochondrial dysfunction triggers a lipodystrophic syndrome with insulin resistance, hepatosteatosis, and cardiovascular complications, *Faseb. J.* 28 (10) (2014) 4408–4419.
- [49] P. Prasun, Role of mitochondria in pathogenesis of type 2 diabetes mellitus, *J. Diabetes Metab. Disord.* 19 (2) (2020) 2017–2022.
- [50] J. Nielsen, et al., Lipid droplet size and location in human skeletal muscle fibers are associated with insulin sensitivity, *Am. J. Physiol. Endocrinol. Metab.* 313 (6) (2017) E721–E730.
- [51] J.D. Covington, et al., Intramyocellular lipid droplet size rather than total lipid content is related to insulin sensitivity after 8 weeks of overfeeding, *Obesity* 25 (12) (2017) 2079–2087.
- [52] T. Shi, F. Wang, E. Stieren, Q. Tong, SIRT3, a mitochondrial sirtuin deacetylase, regulates mitochondrial function and thermogenesis in brown adipocytes, *J. Biol. Chem.* 280 (2005) 13560–13567.
- [53] H. Miki, et al., Essential role of insulin receptor substrate 1 (IRS-1) and IRS-2 in adipocyte differentiation, *Mol. Cell Biol.* 21 (7) (2001) 2521–2532.
- [54] D.S. Fernandez-Twinn, et al., Downregulation of IRS-1 in adipose tissue of offspring of obese mice is programmed cell-autonomously through post-transcriptional mechanisms, *Mol. Metabol.* 3 (3) (2014) 325–333.
- [55] N. Jiang, et al., Cytokines and inflammation in adipogenesis: an updated review, *Front. Med.* 13 (3) (2019) 314–329.
- [56] C. Caër, et al., Immune cell-derived cytokines contribute to obesity-related inflammation, fibrogenesis and metabolic deregulation in human adipose tissue, *Sci. Rep.* 7 (1) (2017) 1–11.
- [57] L. Al-Mansoori, et al., Role of Inflammatory Cytokines, Growth Factors and Adipokines in Adipogenesis and Insulin Resistance, *Inflammation*, 2021, pp. 1–14.
- [58] E. Jarc, T. Petan, A twist of FATE: lipid droplets and inflammatory lipid mediators, *Biochimie* 169 (2020) 69–87.
- [59] C. Kinnear, et al., Form follows function: nanoparticle shape and its implications for nanomedicine, *Chem. Rev.* 117 (17) (2017) 11476–11521.
- [60] J. Pi, et al., Deficiency in the nuclear factor E2-related factor-2 transcription factor results in impaired adipogenesis and protects against diet-induced obesity, *J. Biol. Chem.* 285 (12) (2010) 9292–9300.
- [61] Y. Hou, et al., Nuclear factor erythroid-derived factor 2-related factor 2 regulates transcription of CCAAT/enhancer-binding protein β during adipogenesis, *Free Radic. Biol. Med.* 52 (2) (2012) 462–472.
- [62] B.-R. Kim, et al., Suppression of Nrf2 attenuates adipogenesis and decreases FGF21 expression through PPAR γ in 3T3-L1 cells, *Biochem. Biophys. Res. Commun.* 497 (4) (2018) 1149–1153.

- [63] Q. Ma, L. Battelli, A.F. Hubbs, Multiorgan autoimmune inflammation, enhanced lymphoproliferation, and impaired homeostasis of reactive oxygen species in mice lacking the antioxidant-activated transcription factor Nrf2, *Am. J. Pathol.* 168 (6) (2006) 1960–1974.
- [64] D. Howie, et al., Foxp3 drives oxidative phosphorylation and protection from lipotoxicity, *JCI insight* 2 (3) (2017).
- [65] A.Y. Rudensky, Regulatory T cells and Foxp3, *Immunol. Rev.* 241 (1) (2011) 260–268.
- [66] C.-S. Hsieh, et al., An intersection between the self-reactive regulatory and nonregulatory T cell receptor repertoires, *Nat. Immunol.* 7 (4) (2006) 401–410.